ISSN 0965-545X, Polymer Science, Series A, 2019, Vol. 61, No. 4, pp. 504–513. © Pleiades Publishing, Ltd., 2019.

COMPOSITES

Impact of ZnO Nanoparticles on Thermal Properties of Poly(3-hydroxybutyrate-*co*-10 mol % 3-hydroxyhexanoate) Copolymer

J. Vishnu Chandar[a],*, S. Shanmugan[a], D. Mutharasu[a], and A. A. Azlan[a]

[a]*School of Physics, Universiti Sains Malaysia (USM), Minden, Pulau Pinang, 11800 Malaysia*

** e-mail: vishnuchandar.j@gmail.com*

Received April 20, 2018; revised November 28, 2018; accepted January 17, 2019

Abstract—Biopolymer composites using poly(3-hydroxybutyrate-*co*-10 mol % 3-hydroxyhexanoate) (P(3HB-*co*-10 mol % 3HHx)) and ZnO nanoparticles (NPs) were prepared by solution casting method and the effect of ZnO NPs on thermal properties of the prepared biopolymer composites (P(3HB-*co*-10 mol % 3HHx)/ZnO NPs) were studied using DSC, TGA, GPC, and thermal conductivity analyzer. DSC analysis revealed the dual melting behavior of both neat P(3HB-*co*-10 mol % 3HHx) and its composites. It also showed that the incorporation of ZnO NPs into P(3HB-*co*-10 mol % 3HHx) decreased the melting temperature T_m, but increased the melting enthalpy ΔH_m and degree of crystallinity X_c of the composites. Compared to neat P(3HB-*co*-10 mol % 3HHx), the initial degradation temperature T_{99} of the prepared composites was decreased and vice versa for final degradation temperature due to the addition of ZnO NPs which was revealed from TGA results. The observed thermal conductivity value of neat P(3HB-*co*-10 mol % 3HHx) and its composites were in between ~5.6×10^{-2} and ~7.9×10^{-2} W m/K with the very high value noticed for 30% ZnO NPs reinforced P(3HB-*co*-10 mol % 3HHx) composites. Overall P(3HB-*co*-10 mol % 3HHx)/ZnO NPs composites exhibited high thermal diffusivity and thermal effusivity compared to neat P(3HB-*co*-10 mol % 3HHx) with very high value noted for 30% ZnO NPs and 5% ZnO NPs reinforced P(3HB-*co*-10 mol % 3HHx) composites respectively which is essential for thermal related applications.

DOI: 10.1134/S0965545X19040102

INTRODUCTION

Ecological contamination and the threat of global warming has been drastically increased across the entire planet due to the increased usage of non-biodegradable plastics which is difficult to dispose and recycle [1, 2]. The structure and properties of petroleum based plastics like polypropylene, polystyrene and polyethylene can be easily modified and it is used in manufacturing industries ranging from consumer products to medical, automobile, aircraft, telecommunications equipment, textiles and packaging industry etc. [3–5]. However, petroleum-based plastics are xenobiotic, which are resistant to enzymatic degradation which makes them undesirable. In order to eliminate this growing threat and to reduce the pollution in the environment, many countries are developing a biodegradable material that can be degraded and disintegrated by enzymatic actions of living organism (such as bacteria, fungi etc.) which is obtained from renewable sources [2, 6, 7].

Polyhydroxyalkanoates (PHAs) are biopolyesters synthesized by bacteria in the intracellular region as carbon and energy reserves [8–11] which exhibits properties similar to the thermoplastics such as polypropylene [12, 13] and hence can be used as a substitute for thermoplastics [14]. The first homopolymer and most extensively studied to be discovered from PHA is Poly(3-hydroxybutyrate) [P(3HB)] [15] which is produced by bacterial fermentation method. Though P(3HB) is fully degradable and biocompatible, due to its brittleness, rigidity and high production cost, it couldn't extend its range of applications. Copolymerization of different monomer units with P(3HB) monomer will results in more flexible polymers. The crystallinity, thermal and degradation property can be easily modified by adding different monomer units. In this case, 3HHx monomer units is copolymerized with P(3HB) homopolymer which results in formation of poly(3-hydroxybutyrate-*co*-3-hydroxyhexanoate) [P(3HB-*co*-3HHx)] copolymer. Another approach being reported, where P(3HB) was reinforced with polycaprolactone (PCL), polylactide [16] and hydroxyapatite [17], multi-walled carbon nanotubes [18] and organically modified montmorillonite (OMMT) [19]. Addition of nanofillers into the polymers will not only change the polymer structure but also enhance the physical, thermal and other properties of polymer [20]. Due to the low cost, UV absorption, heat barrier and good thermal conductiv-

ity, noble metal oxide nanoparticles have drawn attention among global researcher's especially ZnO, TiO_2, MgO, and CaO [21]. According to literature [22], ZnO NPs acts as a retarding agent for poly(3-hydroxybutyrate-*co*-3-hydroxyvalerate) (PHBV)/ZnO composite whereas it acts as a nucleating agent for PHB/ZnO NPs composite [23]. Other than this, ZnO NPs were reinforced with poly(vinyl alcohol) (PVA), poly(ethylene oxide) (PEO) [24, 25] and polyethylene terephthalate (PET) [26] through solution casting method and their crystallization behavior, thermal behavior and UV-absorption was studied.

In this work, using solution casting method, ZnO NPs ranging from 0 to 30% were reinforced with P(3HB-*co*-10 mol % 3HHx) copolymer to prepare biopolymer composite films and their thermal properties such as melting point, melting enthalpy, degree of crystallinity, thermal degradation and stability were studied using Differential scanning calorimetry (DSC), thermogravimetric Analysis (TGA) and gel permeation chromatography (GPC) respectively. Thermophysical parameters such as thermal conductivity, volumetric heat capacity, thermal diffusivity and thermal effusivity were studied using thermal conductivity analyzer. The observed results are presented and discussed here in detail to find out whether the addition of ZnO NPs in the P(3HB-*co*-10 mol % 3HHx) copolymer matrix will improve the thermal properties or not.

EXPERIMENTAL

Biosynthesis and Extraction of Poly(3-hydroxybutyrate-co-10 mol % 3-hydroxyhexanoate) [P(3HB-co-10 mol % 3HHx)] Copolymer by Recombinant C. necator Re2058/pCB113

Recombinant *C. necator* Re2058/pCB113 cells were cultured in Nutrient rich (NR) agar plates for 24 h and transferred to NR broth which was then incubated at a constant temperature 30°C for 8 h. Minimal medium with 100 mL capacity were prepared in a shake flask that contains 7 g/L of fructose, 0.54 g/L of urea and 2 g/L of palm olein. These cultured cells were inoculated into the minimal medium and used as inoculum for the fermenter which is equipped with control systems for dissolved oxygen [INFORS HT (Labfors 3), Switzerland], pH, and temperature. The temperature and pH of the culture medium was maintained at 30°C and 7.0 ± 0.1 respectively. Three SiC blade Rushton impeller operating at a speed of 200–900 rpm and 1 VVM air was supplied through filter cartridges (Sartorius Stedim, Germany) and the dissolved oxygen concentration was maintained at above 40%.

In order to sterilize the culture medium together with fermenter Autoclave (HV110, Hiryama, Japan) was used, which was maintained at 121°C for 30 min. Freeze dried cells were mixed in chloroform with the ratio of 1 g: 100 mL and 5 days continuous stirring was provided at the room temperature. Then the cell debris was removed, and the filtered solution was concentrated by using a rotary evaporator. The concentrated solution was added drop-wise into vigorously stirred chilled methanol for 1 h to precipitate and purify the polymer. Then the extracted and purified polymer was used for experiments.

Preparation of Neat PHB-10HZ0 and Biopolymer Composite (PHB-10HZ0/ZnO NPs) Films

Extracted and purified P(3HB-*co*-10 mol % 3HHx) copolymer weighs about 500 mg was dissolved in chloroform solvent together with 6 different concentration of ZnO NPs ranging from 5 to 30% (25–150 mg) and stirred using mechanical stirrer until a homogeneous colloidal solution was obtained which was then sonicated for 30 min. Then the solution was casted in Petri dish with 55 mm diameter at room temperature for 48 h. After 48 h, the films were retrieved from the Petri dish and the retrieved films were observed with thickness around 0.3 mm and diameter of about 50 mm. The sample name throughout this manuscript is given based on the information provided in Table 1. Hereafter, the short form will be used for discussion.

Thermal Characterization of Neat PHB-10HZ0 and Biopolymer Composite (PHB-10HZ0/ZnO NPs) Films

Differential scanning calorimetry (DSC) analysis. The thermal properties of the neat PHB-10HZ0 and PHB-10HZ0/ZnO NPs composite films were determined by Differential scanning calorimetry (DSC, Shimadzu, Japan) experiments under nitrogen environment. 4 mg of samples were heated from room temperature to 180°C at a step rate of grad/min and kept at 180°C for 5 min to erase the thermal history of the material which was then cooled to room temperature and then again reheated to 180°C with constant step rate of 5 deg/min.

Gel permeation chromatography (GPC). In order to determine the molar mass and mass distributions of polymer samples, Gel permeation chromatography is the most widely acceptable technique. It was used to determine the molar mass related parameters of neat PHB-10HZ0 and PHB-10HZ0/ZnO NPs composite films in this work. In order to prepare 1 mg/mL concentration solution, 3 mg of PHB-10HZ0 copolymer and 3 mg of PHB-10HZ0/ZnO NPs composite samples were dissolved in 3 mL chloroform separately and filtered through 0.45 μm PTFE syringe filter. The prepared samples were injected at a volume of 50 μL into an Agilent liquid chromatograph equipped with an auto sampler, column oven, and refractive index detector (RID). Molar mass of the samples were determined by using Shodex GPC K-802 and K-806M. Chloroform was used as a mobile phase at

Table 1. Sample information and naming

Sample composition	Total weight = weight of poly[3-hydroxybutyrate-*co*-10 mol % 3-hydroxyhexanoate] copolymer + ZnO nanoparticles	Abbreviated name of the sample
P(3HB-*co*-10 mol % 3HHx)	500 mg	PHB-10HZ0
P(3HB-*co*-10 mol % 3HHx)+ 5% ZnO	475 + 25 mg	PHB-10HZ5
P(3HB-*co*-10 mol % 3HHx) + 10% ZnO	450 + 50 mg	PHB-10HZ10
P(3HB-*co*-10 mol % 3HHx) + 15% ZnO	425 + 75 mg	PHB-10HZ15
P(3HB-*co*-10 mol % 3HHx) + 20% ZnO	400 + 100 mg	PHB-10HZ20
P(3HB-*co*-10 mol % 3HHx) + 25% ZnO	375 + 125 mg	PHB-10HZ25
P(3HB-*co*-10 mol % 3HHx) + 30% ZnO	350 + 150 mg	PHB-10HZ30

the rate of 1 mL/min. The column oven was maintained at 40°C. To generate the calibration curve, polystyrene standards with low molar mass dispersity $Đ_M$ were used. By comparing peak retention time with polystyrene standards of known molar mass in Agilent software, molar mass M_w, molar number M_n, and $Đ_M$ values of the prepared samples were determined.

Thermogravimetric analysis (TGA). The effect of ZnO NPs on the thermal degradation and stability of the prepared samples were determined by using Thermo Gravimetric (PERKIN ELMER/STA 6000) Analyzer. Approximately 10 mg of each sample was heated in the range of 50 to 900°C at a constant heating rate of 10 deg/min under nitrogen gas environment.

Thermal conductivity analyzer. HotDisk thermal conductivity analyzer (Hot Disk—TPS 2500 S) was used to determine the thermal conductivity, specific heat capacity and thermal diffusivity of neat PHB-10HZ0 and PHB-10HZ0/ZnO NPs composite films at room temperature.

RESULTS AND DISCUSSIONS

Analysis of Thermal Properties of Neat PHB-10HZ0 and PHB-10HZ0/ZnO NPs Composites

In general, addition of nanoparticles into polymers not only alters the crystallinity but also the surface of the polymer which in turn affects the thermal, physical, biodegradability and other properties of the polymer material [18, 23].

Differential Scanning Calorimetry (DSC) Analysis

The effect of ZnO NPs on the thermal properties of PHB-10HZ0 copolymer was evaluated using the DSC analysis, since the study of thermal properties of polymer composites is of great interest. Figure 1 shows the second heating scans of neat PHB-10HZ0 and ZnO NPs reinforced PHB-10HZ0 composites. Melting temperature T_m and enthalpy of melting ΔH_m of neat PHB-10HZ0 and ZnO reinforced PHB-10HZ0 composites were determined from the graph (Fig. 1) and enumerated in Table 2.

It is clear from Fig. 1 that both neat PHB-10HZ0 and ZnO NPs reinforced PHB-10HZ0 composites shows dual melting endothermic peaks. Normally the melting temperature of the PHB is around 175 to 177°C [27, 28] and the addition of 3HHx monomer units decreases the melting temperature due to the presence and bulky nature of propyl side groups which excludes the 3HHx from being co-crystallized with 3HB into the crystalline domains [27]. In this case, neat PHB-10HZ0 shows a strong melting endothermic peak (T_{m1}) at 156.8°C and weak melting endothermic peak (T_{m2}) at 164.3°C. The presence of HHx monomer units results in the distribution of hydroxybutyrate (HB) sequences with different length, which is responsible for the multiple melting behavior of neat PHB-10HZ0 [29]. The first endothermic peak is ascribed to the melting of the crystals formed during the primary crystallization and the second endothermic peak corresponds to melting of the crystals formed from recrystallization during the heating process [30]. Similarly, PHB-10HZ5 shows a very strong peak at 156.9 and 164.0°C compared to neat PHB-10HZ0 whereas all other composites show a weak endothermic peak nearly at 151°C and strong endothermic peak nearly at 162°C. Strong peak observed at 156.9°C shifted to lower temperature and the weak peak exhibited around 164.0°C also shifted to lower temperature for higher loadings of ZnO NPs. According to the literature [31, 32], this dual melting behavior of the composites may be due to compositional heterogeneity, multiple crystalline forms or melting-recrystallization-remelting (MRR). The first melting peak observed around 151°C for composites may be due to the melting of secondary crystallites and there is much

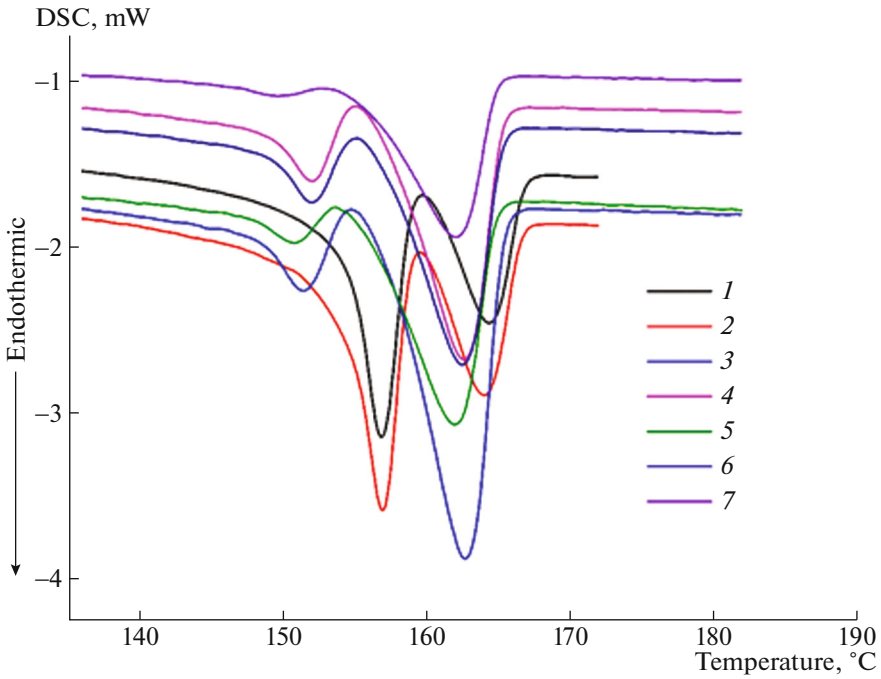

Fig. 1. (Color online) DSC second heating scans of (*1*) neat PHB-10HZ0 and biopolymer composites (PHB10HZ0/ZnO NPs): (*2*) PHB-10HZ5, (*3*) PHB-10HZ10, (*4*) PHB-10HZ15, (*5*) PHB-10HZ20, (*6*) PHB-10HZ25, and (*7*) PHB-10HZ30.

more secondary crystallization in the composites due to the addition of ZnO NPs compared to the neat PHB-10HZ0 during the cooling run or the earlier stage in the second heating run. The secondary crystalline phase melts at lower T_m (151°C), crystallizes, and remelts again at higher T_m (162°C) [22, 23]. Overall the higher loadings of nanoparticles (>5% ZnO NPs) further decrease the melting temperature of the PHB-10HZ0 copolymer.The decrease in T_m may be due to low melt viscosity property of ZnO NPs compared to PHB-10HZ0 copolymer [33]. This is in agreement with the results observed for PHB/Wood flours composites [12].

The enthalpy of melting ΔH_m defines the energy required for the phase change from solid to liquid without a change in temperature and it determines the degree of crystallinity X_c which is an important parameter that determines the mechanical properties of the material [34]. The degree of crystallinity X_c of the prepared samples were determined through the melting enthalpy ΔH_m of the prepared samples and the melting

Table 2. Thermal parameters obtained from DSC thermograms for neat PHB-10HZ0 and biopolymer composites (PHB10HZ0/ZnO NPs)

Sample Name	Melting temperature (T_{m1}/T_{m2}), °C	Enthalpy of melting ($\Delta H_{M,PHB}$), J/g	$X_{c,PHB}$, %
PHB-10HZ0	156.9/164.3	21.3	29.0
PHB-10HZ5	156.9/164.0	18.6	26.8
PHB-10HZ10	151.4/162.7	34.0	51.5
PHB-10HZ15	152.0/162.5	28.2	45.3
PHB-10HZ20	150.7/161.9	27.2	46.3
PHB-10HZ25	151.9/162.5	27.7	50.3
PHB-10HZ30	149.6/162.0	21.0	40.9

$X_{c,PHB}$—degree of crystallinity with respect to PHB-10HZ0 copolymer weight fraction in the composites.
T_{m1}—first endothermic melting temperature, T_{m2}—second endothermic melting temperature.

enthalpy of 100% crystalline PHB ($\Delta H^{\circ}_{M,PHB}$). With respect to the weight ratio of PHB-10HZ0 copolymer and ZnO NPs, the degree of crystallinity was determined using the following equation [23] and the resultant data's are summarized in Table 2.

$$X_{c,PHB} = \Delta H_{M,PHB}/(\Delta H^{\circ}_{M,PHB} * W_{PHB}), \quad (1)$$

where $X_{c,PHB}$ is the degree of crystallinity with respect to weight fraction of PHB-10HZ0 copolymer, W_{PHB} is the weight of PHB-10HZ0 copolymer in the composites, $\Delta H_{M,PHB}$ is the melting enthalpy of neat PHB-10HZ0 and PHB-10HZ0/ZnO NPs composites and $\Delta H^{\circ}_{M,PHB}$ is the theoretical value of enthalpy for a 100% crystalline sample (146.6 J/g) [35, 36]. From Table 2, neat PHB-10HZ0 samples exhibit ΔH_m value at around 21.3 and upon addition of 5% ZnO NPs, ΔH_m value decreases to 18.6 and then increases again with very high value (34.0) for PHB-10HZ10 composite sample. Overall the addition of ZnO NPs altered the melting enthalpy which in turn directly affects the degree of crystallinity X_c. The degree of crystallinity X_c also follows the same trend like melting enthalpy ΔH_m with very low value observed for PHB-10HZ5 (26.7%) composite and neat PHB-10HZ0 (29.0%). Brittle polymers usually have high crystallinity which narrows the range of applications. In this case PHB-10HZ10 and PHB-10HZ25 exhibit very high X_c (51.5 and 50.3%) compared to neat PHB-10HZ0 (29%) and other composites which indicates that PHB-10HZ10 and PHB-10HZ25 composites are highly brittle polymer. Neat PHB-10HZ0 and other composites exhibit X_c in the range of less brittle polymer materials such as PHBV/PCL blend which exhibit X_c value around 46.0% [37]. Overall the addition of ZnO NPs decreases the melting temperature T_m whereas it increases both the melting enthalpy ΔH_m and degree of crystallinity X_c. Depends upon the polymer material, ZnO NPs acts as a nucleating agent [14, 23] and retarding agent [22], in this case ZnO NPs acts both as a retarding agent in the case of melting temperature whereas it acts as a nucleating agent for melting enthalpy and degree of crystallinity.

Gel Permeation Chromatography Analysis

Gel permeation chromatography is the analytical technique used to determine the mass-average molar mass M_w and number-average molar mass M_n and Molar mass distribution which are all important parameters since it changes the physical properties of the polymer significantly. From batch to batch, all the above mentioned parameters varies with respect to substrate and conditions involved in the cell culture [38]. This shows that GPC results of neat PHB-10HZ0 copolymer obtained from this cell culture and preparation method might differ from other polymers with different culture conditions. Molar mass dispersity $Đ_M$ measures the broadness or narrowness of the molar mass distribution in a polymer and is calculated from the following equation [39, 40] and summarized in Table 3:

Table 3. Mass-average molar mass M_w, number-average molar mass M_n and molar mass dispersity $Đ_M$ data obtained from GPC analysis for neat PHB-10HZ0 and biopolymer composites (PHB-10HZ0/ZnO NPs)

Sample Name	$M_w \times 10^3$	$M_n \times 10^3$	$Đ_M$
PHB-10HZ0	5.9 ± 0.5	3.3 ± 0.0	1.8 ± 0.1
PHB-10HZ5	6.1 ± 0.5	3.3 ± 0.0	1.9 ± 0.2
PHB-10HZ10	4.3 ± 0.2	1.3 ± 0.1	3.3 ± 0.4
PHB-10HZ15	6.7 ± 1.3	3.0 ± 0.1	2.2 ± 0.5
PHB-10HZ20	7.0 ± 0.7	2.5 ± 0.1	2.8 ± 0.2
PHB-10HZ25	6.9 ± 0.9	2.5 ± 0.2	2.8 ± 0.5
PHB-10HZ30	7.8 ± 1.6	3.2 ± 0.1	2.5 ± 0.6

$$Đ_M = M_w/M_n. \quad (2)$$

It is known that M_n is less than M_w for all synthetic polydisperse polymers [41] and it is clear from Table 3 that both neat PHB-10HZ0 and its composites attain a low M_n than M_w. Addition of ZnO NPs altered both M_w and M_n values. Overall the M_w value increases with increases in ZnO NPs concentration with a very high value observed for PHB-10HZ30 composite except PHB-10HZ10 and M_n value decreases with increase in ZnO NPs concentration except PHB-10HZ5. Molar mass dispersity $Đ_M$ of ZnO NPs reinforced PHB-10HZ0 composites is greater than neat PHB-10HZ0 with very high value observed for PHB-10HZ10 composite. Addition of ZnO NPs increased the dispersity of PHB-10HZ0 copolymer. The increase in molar mass dispersity (i.e. $Đ_M > 1$) indicates the broadness of the polymer. According to the data mentioned in Table 3, the prepared composite samples shows high molar mass dispersity compared to commercial PHB homopolymer [39, 42] and PHB-10HZ0 copolymer [43] whereas the prepared neat PHB-10HZ0 sample shows low values. High molar mass polymers usually crystallize more slowly which leads to the formation of smaller crystals and lower degree of crystallinity [39]. From Table 3, neat PHB-10HZ0 has high molar mass and low molar mass dispersity than composites which may be associated to low degree of crystallinity whereas PHB-10HZ10 composite sample exhibit low M_w and high $Đ_M$ compared to neat PHB-10HZ0 and other composites, which may be attributed to high degree of crystallinity observed in the DSC analysis.

Thermogravimetric Analysis

Thermal degradation of polymer involves heating the polymer under nitrogen environment which changes the molecular weight, optical and other prop-

Table 4. Thermal degradation and stability parameters obtained from TGA and DTG thermograms for neat PHB-10HZ0 and biopolymer composites (PHB-10HZ0/ZnO NPs)

Sample name	T_{99}, °C	T_{50}, °C	T_f, °C	CR, %	T_{DP}, °C
PHB-10HZ0	272.1	302.5	330.2	0.2 ± 0.02	303.48
PHB-10HZ5	265.9	286.4	557.4	4.5 ± 0.1	285.2, 414.6
PHB-10HZ10	266.4	291.2	525.6	7.9 ± 0.1	287.6, 424.3
PHB-10HZ15	265.1	296.2	601.4	12.9 ± 0.1	284.5, 414.8
PHB-10HZ20	257.4	290.9	579.5	12.5 ± 0.1	282.9, 417.5
PHB-10HZ25	263.7	317.9	631.9	20.5 ± 0.1	283.9, 415.8
PHB-10HZ30	265.5	388.8	661.9	33.2 ± 0.1	281.9, 354.2, 413.9

T_{99}—initial degradation temperature at 1% mass loss, T_{50}—degradation temperature at 50% mass loss, T_f—final degradation temperature, CR—char residue, T_{DP}—derivative peak temperature.

erties due to molecular deterioration. Thermal stability determines the polymer material's resistance to degradation. The effect of ZnO NPs on the degradation rate and thermal stability of PHB-10HZ0 copolymer was analyzed by thermo gravimetric analyzer. A graph of weight loss against temperature and its derivate graph (DTG) was plotted from the data obtained from the TGA equipment. Figures 2a and 2b show the TGA and DTG thermograms of neat PHB-10HZ0 and PHB-10HZ0/ZnO NPs composites. It is clear from Fig. 2a, neat PHB-10HZ0 show one step degradation whereas ZnO NPs reinforced PHB-10HZ0 composites exhibits more than one step degradation which shows the effect of ZnO NPs on the thermal degradation and stability of PHB-10HZ0 copolymer. In order to analyze the effect of ZnO NPs on the thermal degradation and stability in detail, three different temperature readings T_{99}, T_{50}. T_f were taken from the thermogram (Fig. 2a) and summarized in Table 4.

T_{99} refers to initial degradation temperature at 1% mass loss, T_{50} refers to temperature at 50% mass loss and T_f refers to final degradation temperature which determines the thermal stability of the PHB-10HZ0 copolymer. From Table 4, it is clear that the PHB-10HZ0 exhibit initial degradation temperature around ~272°C which is decreasing to ~265°C for PHB-10HZ5 composite sample and then the temperature remains around ~263 to ~266°C for all other composites except PHB-10HZ20 composite sample which exhibit T_{99} around ~257°C. Overall the addition of ZnO NPs decreases the initial degradation temperature (T_{99}). Neat PHB-10HZ0 exhibit one step degradation that starts at ~272°C and shows maximum degradation rate at around 330°C. This degradation may be due to the production of shorter chain fragments with carboxylic terminal groups and crotonic acid as by-products from random chain scission mechanism [44]. The T_{50} of the neat PHB-10HZ0 starts at ~302°C and then decreases to ~286°C upon addition of 5% ZnO NPs in the PHB-10HZ0 copolymer and then gradually increases with increasing ZnO NPs concentration with a maximum temperature observed for PHB-10HZ30 composite sample. Overall the higher loadings of ZnO NPs i.e. (>20% ZnO NPs) has increasing effect whereas for all other concentrations, T_{50} of composites is lower than neat PHB-10HZ0. Coming to T_f, incorporation of ZnO NPs shows a positive effect that the T_f of the neat PHB-10HZ0 is lower than the T_f of the ZnO reinforced PHB-10HZ0 composites.

This behavior is probably because the added ZnO NPs acts as a heat barrier, which improves the heat resistance of the PHB-10HZ0 copolymer matrix. Moreover, it also facilitates heat dissipation inside the composite matrix which resulted in the increment of thermal stability due to high thermal conductivity property of ZnO NPs [45]. Like this, the increment in the final degradation temperature was observed in PHB/OMMT composites [46]. Due to incomplete combustion, certain solid materials when subjected to high temperature results in chemical residue i.e. char residue (CR). In this case, addition of ZnO NPs increased the char residue content and the resultant CR values are taken from the thermogram (Fig. 2a) and summarized in Table 4. Inorganic residues are formed due to the incorporation of additives (ZnO NPs) which resulted in the formation of glassy layer that is impenetrable to volatiles produced in the thermal decomposition process and protect the underlying layer from thermal breakdown which in turn increases the thermal stability [47].

Derivative thermogram (DTG) is the derivative of TGA thermogram which shows the temperature of maximum rate of weight loss. Figure 2b shows the DTG thermogram of neat PHB-10HZ0 and PHB-10HZ0/ZnO NPs composites. It is clear from Fig. 2b that a single peak is found for neat PHB-10HZ0 whereas more than one peak is found for all the com-

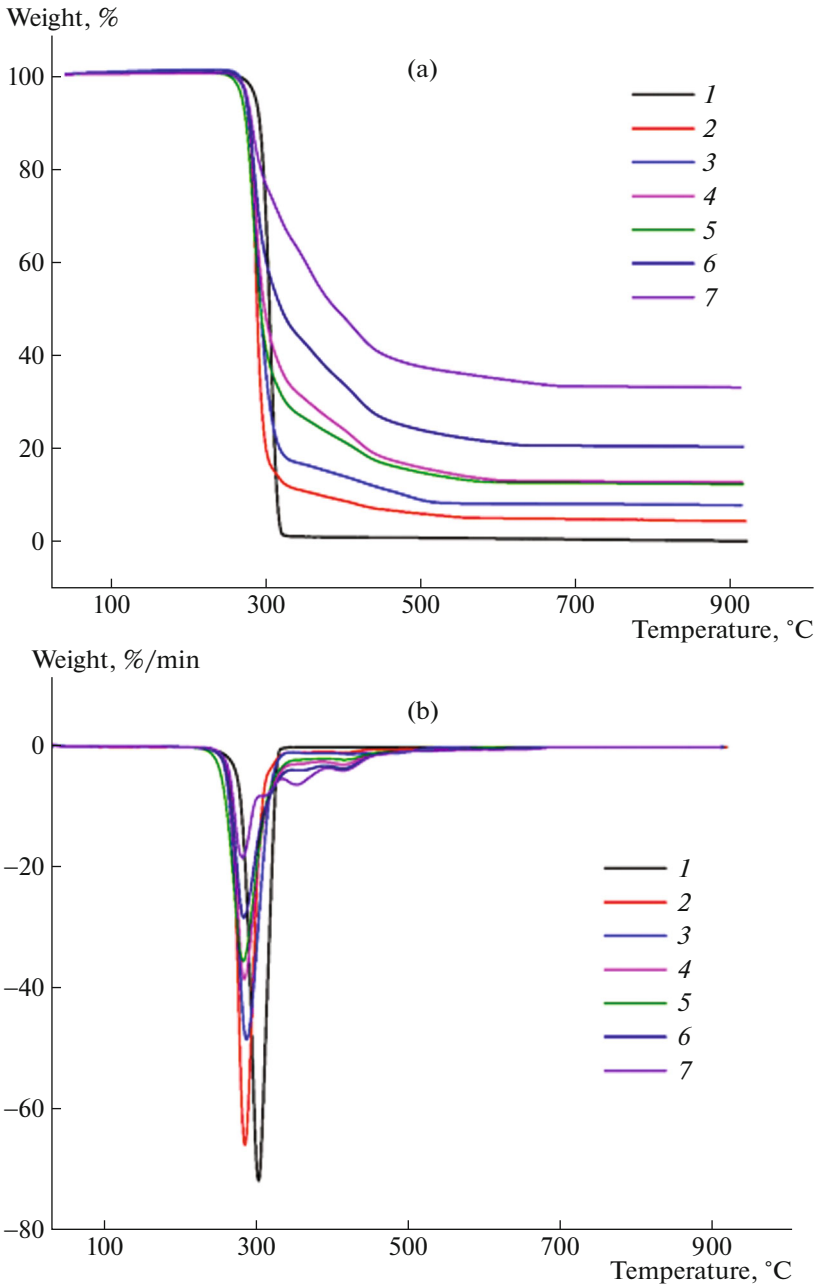

Fig. 2. (Color online) (a) TGA and (b) DTG thermogram of (*1*) neat PHB-10HZ0 and biopolymer composites (PHB-10HZ0/ZnO NPs): (*2*) PHB-10HZ5, (*3*) PHB-10HZ10, (*4*) PHB-10HZ15, (*5*) PHB-10HZ20, (*6*) PHB-10HZ25, and (*7*) PHB-10HZ30.

posites which indicates that neat PHB-10HZ0 exhibit one step degradation and PHB-10HZ0/ZnO NPs composites show dual or three step degradations. Neat PHB-10HZ0 display maximum weight loss at ~303°C whereas the composites demonstrate maximum weight loss at dual temperature around ~285 and 414°C except PHB-10HZ30 composite sample which has three peaks at ~281, 354, and 413°C respectively. For some polymer materials, addition of ZnO NPs may rise the initial degradation temperature T_{99} [23], in this case ZnO NPs decreases the T_{99} and increases the final degradation temperature T_f which improves the thermal stability of the PHB-10HZ0 copolymer.

Thermophysical Parameter Analysis

Thermal conductivity analysis. Thermal conductivity determines the materials ability to conduct heat. In order to analyze the effect of ZnO NPs on the thermal conductivity of PHB-10HZ0 copolymer, thermal

Table 5. Thermophysical parameters of neat PHB-10HZ0 and biopolymer composites (PHB-10HZ0/ZnO NPs)

Sample name	Thermal conductivity, W/(m K)	Volumetric heat capacity, MJ/(m^3 K)	Thermal diffusivity, mm^2/s	Thermal effusivity, W s$^{1/2}$/(m^2 K)
PHB-10HZ0	0.05699	0.6608	0.0863	0.1941
PHB-10HZ5	0.05968	1.031	0.0579	0.2481
PHB-10HZ10	0.05972	0.6463	0.0924	0.1965
PHB-10HZ15	0.06032	0.5789	0.1042	0.1869
PHB-10HZ20	0.074	0.7143	0.1036	0.2299
PHB-10HZ25	0.06006	0.4977	0.1207	0.1729
PHB-10HZ30	0.07908	0.536	0.1475	0.2059

conductivity of neat PHB-10HZ0 and PHB-10HZ0/ZnO NPs composites films were measured and summarized in Table 5.

The observed thermal conductivity value of neat PHB-10HZ0 and its composites were in between 5.6×10^{-2} and 7.9×10^{-2} W m/K. It is clear from Table 5, addition of ZnO NPs in the polymer matrix clearly influences and increase the thermal conductivity of PHB-10HZ0 copolymer based on the concentration of ZnO NPs. PHB-10HZ30 composite sample exhibit high thermal conductivity (7.9×10^{-2} W m/K) than all other composites and neat PHB-10HZ0. The thickness of the samples also plays a very crucible role in controlling the thermal conductivity of PHB-10HZ0 copolymer. Due to the anisotropy of the thin films, the thermal conductivity of prepared films may differ from those of bulk polymer materials [48]. The prepared composite films attain a very low thermal conductivity compared to the thermal conductivity of commercial thermoplastics like polypropylene, polystyrene (0.11, 0.14) [49] which may be due to the thickness of the prepared films (0.3 mm thickness). The crystallinity of the material also determines the thermal conductivity of the polymer. Generally, the thermal conductivity of the polymers depends on polymer chain segment orientation. Compared to amorphous polymers, crystalline polymers have highly ordered chain segments which results in higher heat transportation ability than amorphous ones [50, 51]. According to the unpublished work from the same author group, overall the addition of ZnO NPs increases the PHB-10HZ0 copolymer's amorphous nature except for PHB-10HZ20 composite where it increases the crystallinity of the polymer, but the intensity of ZnO NPs related peaks are relatively much higher than the polymer related peaks. The main reason behind the thermal conductivity increment is due to the ZnO NPs related peak intensity and its high crystallinity. The thermal conductivity of ZnO NPs (22 (W m)/K) [52] is high, which increases the thermal conductivity of PHB-10HZ0/ZnO NPs composites compared to neat PHB-10HZ0. However, still the conductivity of the prepared composites is relatively low (i.e., <0.1 (W m)/K). This may be due to the presence of interfacial thermal resistance between the ZnO NPs and the PHB-10HZ0 copolymer matrix. Generally, to transfer the heat, energy needs to be transported from one place to another. For example, diffusion and advection are the only means to transport the energy in liquids. Like that, phonons and electrons are the primary transportation for solids. Phonons are nothing but quantized modes of vibrational energy in periodic solids (i.e. rigid crystal lattice) and it is the only transportation to conduct the heat in most of the polymer matrix since free electron movement is not possible in polymer [53] and due to numerous defects which leads to scattering of phonons may also result in low thermal conductivity polymers [54]. In order to further improve the thermal conductivity, PHB-10HZ0 copolymer needs to be reinforced with high thermal conductivity nanofillers such as carbon nanotubes, graphite etc.

Thermal diffusivity. Thermal diffusivity α depends on thermal conductivity k, density ρ and specific heat capacity C_p and their inter-relationship is explained by the following equation [55]:

$$\alpha = k/\rho C_p. \quad (3)$$

The thermal diffusivity of neat PHB-10HZ0 and PHB-10HZ0/ZnO NPs composites were obtained and summarized in Table 5. According to [56], a material with high thermal conductivity, low density and low heat capacity can achieve high thermal diffusivity. This is in agreement with the obtained results. PHB-10HZ5 composite sample with thermal conductivity of ~0.05968 W m/K and *vhc* around 1.031 MJ/(m^3 K) achieved a very low diffusivity value of about ~0.05788 mm^2/s whereas PHB-10HZ30 exhibit very high thermal diffusivity value around ~0.1475 mm^2/s. The observed values (~0.05–0.15 mm^2/s) are high compared to the existing non-degradable thermoplastic like polyvinyl chloride (0.08 mm^2/s) [57], polypropylene (0.096 mm^2/s) [58], polytetrafluoroethylene (0.124 mm^2/s) [59] and polycarbonate (0.144 mm^2/s) [58].

Thermal effusivity. The thermal effusivity of the material is a measure of its ability to exchange heat

with the surrounding and varies due to their differing ability to transfer heat. The thermal effusivity of neat PHB-10HZ0 and its composites are calculated from the following equation [27] and the resultant values are enumerated in Table 5.

$$e = \sqrt{k\rho C_p}. \quad (4)$$

In general, as the surrounding temperature drops, a material with high thermal diffusivity will quickly dissipate the heat from its surface (cannot hold heat much longer) and vice versa for material with low thermal diffusivity. Like *vhc*, PHB-10HZ5 composite sample exhibit very high thermal effusivity (~0.2481 $W s^{1/2}/(m^2 K)$) that may be related to quick heat dissipation compared to neat PHB-10HZ0 and all other composites.The differences in heat transfer through and between PHB-10HZ0 copolymer and ZnO NPs may be attributed to the changes in the values of thermal effusivity. Overall addition of ZnO NPs in the polymer matrix results in the increase of thermal effusivity compared to neat PHB-10HZ0.

CONCLUSIONS

Neat P(3HB-*co*-10 mol % 3HHx) and P(3HB-*co*-10 mol % 3HHx)/ZnO nanoparticles (NPs) composites were prepared by solution casting method and the effects of ZnO NPs on the thermal properties and thermo physical parameters have been investigated. DSC results confirmed that the addition of ZnO NPs decrease the melting temperature and increase the melting enthalpy and degree of crystallization of P(3HB-*co*-10 mol % 3HHx)/ZnO NPs composites. Dual melting behavior was observed for both neat P(3HB-*co*-10 mol % 3HHx) and its composites. ZnO NPs acts as a nucleating agent which enhanced the thermal conductivity, thermal diffusivity and thermal effusivity of P(3HB-*co*-10 mol % 3HHx)/ZnO NPs composites compared to neat P(3HB-*co*-10 mol % 3HHx). Overall the addition of ZnO NPs increased the thermal stability of the P(3HB-*co*-10 mol % 3HHx) copolymer. On considering the thermal analysis, it clearly shows that lower % of ZnO NPs may not be a suitable filler material for P(3HB-*co*-10 mol % 3HHx) copolymer. But higher % of ZnO NPs increases the thermal conductivity and stability. Therefore, higher loadings i.e. ≥25% ZnO NPs may be used for low temperature applications which require high thermal stability. However, from the above analysis, it is concluded that in order to further improve the thermal properties of the PHB-10HZ0 copolymer, high thermal conductivity nanofillers such as CNTs, graphite should be reinforced with PHB-10HZ0 copolymer.

ACKNOWLEDGMENTS

Vishnu Chandar Janakiraman expresses gratitude to USM Fellowship for financial support. Authors wishes to acknowledge Murugan Paramasivan, PhD and Dr. Sudesh Kumar, School of biological sciences in USM main campus for providing the P(3HB-*co*-10 mol % 3HHx) copolymer material and facilities such as DSC and GPA for experimental works. In addition to that, School of Chemical Sciences, USM Main campus also provided facilities to study TGA.

REFERENCES

1. G. E. Luckachan and C. Pillai, J. Polym. Environ. **19**, 637 (2011).
2. I. Vroman and L. Tighzert, Materials (Basel) **2**, 307 (2009).
3. *Feedstock Recycling of Plastic Wastes,* Ed. by J. Aguado and D. P. Serrano (Royal Soc. Chem., Cambridge, 2007).
4. C. Reddy, R. Ghai, and V. C. Kalia, Bioresour. Technol. **87**, 137 (2003).
5. K. Petersen, P. V. Nielse, and G. Bertelsen,Trends Food Sci.Technol. **10**, 52 (1999).
6. T. Aminabhavi, R. Balundgi, and P. Cassidy, Polym.-Plast. Technol. Eng. **29**, 235 (1990).
7. M. Avella, J. J. De Vlieger, M. E. Errico, S. Fischer, P. Vacca, and M. G. Volpe, Food Chem. **93**, 467 (2005).
8. S. Y. Lee, Biotechnol. Bioeng. **49**, 1 (1996).
9. A. Steinbüchel, in *Biomaterials,* Ed. by D. Byrom (MacMillan, New York, 1991), p. 123.
10. S. Song, S. Hein, and A. Steinbüchel, Biotechnol. Lett. **21**, 193 (1999).
11. L. L. Madison and G. W. Huisman, Microbiol. Mol. Biol. Rev. **63**, 21 (1999).
12. C. S. Wu, J. Appl. Polym. Sci. **102**, 3565 (2006).
13. *Chemistry and Technology of Biodegradable Polymers,* Ed. by G. J. Griffin (Blackie Academic and Professional, London, 1994).
14. M. Sanchez-Garcia, E. Gimenez, and J. Lagaron, Carbohydr. Polym. **71**, 235 (2008).
15. S. Khanna and A. K. Srivastava, Process Biochem. **40**, 627 (2005).
16. *Polyhydroxyalkanoates—Plastic Materials of the 21st Century: Production, Properties, Applications,* Ed. by T. Volova (Nova Publ., UK, 2004).
17. M. Sadat-Shojai, M.-T. Khorasani, A. Jamshidi, and S. Irani, Mater. Sci. Eng. C **33**, 2776 (2013).
18. C. Xu and Z. Qiu, Polym. Adv. Technol. **22**, 538 (2011).
19. M. Erceg, T. Kovačić, and I. Klarić, in *Proceedings of "Fourth International Symposium on Nanostructured and Functional Polymer Based Materials and Nanocomposites", Rome, Italy, 2008* (Rome, 2018).
20. M. Kurian, A. Dasgupta, M. E. Galvin, C. R. Ziegler, and F. L. Beyer, Macromolecules **39**, 1864 (2006).
21. A. M. Nafchi, R. Nassiri, S. Sheibani, F. Ariffin, and A. Karim, Carbohydr. Polym. **96**, 233 (2013).
22. W. Yu, C.-H. Lan, S.-J. Wang, P.-F. Fang and Y.-M. Sun, Polymer **51**, 2403 (2010).
23. A. M. Díez-Pascual and A. L. Díez-Vicente, Int. J. Mol. Sci. **15**, 10950 (2014).

24. J. Lee, D. Bhattacharyya, A. Easteal, and J. Metson, Curr. Appl. Phys. **8**, 42 (2008).
25. H.-M. Xiong, X. Zhao, and J.-S. Chen, J. Phys. Chem. B **105**, 10169 (2001).
26. J. He, W. Shao, L. Zhang, C. Deng, and C. Li, J. Appl. Polym. Sci. **114**, 1303 (2009).
27. Y. Doi, S. Kitamura, and H. Abe, Macromolecules **28**, 4822 (1995).
28. P. King, J. Chem. Technol. Biotechnol. **32**, 2 (1982).
29. Z. Gan, K. Kuwabara, H. Abe, and Y. Doi, in *Biodegradable Polymers and Plastics,* Ed. by E. Chiellini and R. Solaro (Springer, US, 2003), p. 167.
30. Y. Hu, J. Zhang, H. Sato, I. Noda, and Y. Ozaki, Polymer **48**, 4777 (2007).
31. C. Chen, M. K. Cheung, and P. H. Yu, Polym. Int. **54**, 1055 (2005).
32. L. Gunaratne, R. Shanks, and G. Amarasinghe, Thermochim. Acta **423**, 127 (2004).
33. L. Averous, L. Moro, P. Dole, and C. Fringant, Polymer **41**, 4157 (2000).
34. Y. Kong and J. Hay, Polymer **43**, 184 (2002).
35. Y. He, T. Masuda, A. Cao, N. Yoshie, Y. Doi, and Y. Inoue, Polym. J. **31**, 184(1999).
36. Z. Zheng, F.-F. Bei, H.-L. Tian, and G.-Q. Chen, Biomaterials **26**, 3537 (2005).
37. Y. Chun and W. N. Kim, Polymer **41**, 2305 (2000).
38. G.-Q. Chen and W. J. Page, Biotechnol. Lett. **16**, 155 (1994).
39. F. C. Oliveira, M. L. Dias, L. R. Castilho, and D. M. Freire, Bioresour. Technol. **98**, 633 (2007).
40. R. Gilbert, M. Hess, A. Jenkins, R. Jones, P. Kratochvil, and R. Stepto, Pure Appl. Chem. **81**, 31 (2009).
41. *Principles of Polymer Chemistry,* Ed. by A. Ravve (Springer Science and Business Media, New York, 2013).
42. N. Galego, C. Rozsa, R. Sánchez, J. Fung, A. A. Vázquez, and J. Santo Tomás, Polym. Test. **19**, 485 (2000).
43. Q. Liao, PhD Thesis (Stanford University, Stanford, 2010).
44. N. Grassie, E. Murray, and P. Holmes, Polym. Degrad. Stab. **6**, 127 (1984).
45. Z. X. Huang, Z. A. Tang, J. Yu, and S. Bai, Phys. B (Amsterdam, Neth) **406**, 818 (2011).
46. K. Prakalathan, S. Mohanty, and S. K. Nayak, Polym. Compos. **35**, 999 (2014).
47. *SFPE Handbook of Fire Protection Engineering,* Ed. by C. L. Beyler and M. M. Hirschler (Natl. Fire Protecti. Assoc., Quincy; Soc. Fire Protect. Eng., Bethesda, 2002).
48. K. Kurabayashi, M. Asheghi, M. Touzelbaev, and K. E. Goodson, J. Microelectromech. Syst. **8**, 180 (1999).
49. C. T'Joen, Y. Park, Q. Wang, A. Sommers, X. Han and A. Jacobi, Int. J. Refrig. **32**, 763 (2009).
50. *Handbook of Multiphase Polymer Systems,* Ed. by A. Boudenne, L. Ibos, Y. Candau, and S. Thomas (Wiley Online Library, 2011).
51. D. M. Price and M. Jarratt,Thermochim. Acta **392**, 231 (2002).
52. G. Becker, C. Lee, and Z. Lin, Adv. Packag. **14**, 14 (2005).
53. *Handbook of Heat Transfer,* Ed. by W. M. Rosenhow, J. P. Hartnett, and Y. I. Cho (McGraw-Hill, New York, 1998).
54. Y. Agari, A. Ueda, Y. Omura, and S. Nagai, Polymer **38**, 801 (1997).
55. *CRC Handbook of Chemistry and Physics,* Ed by D. R. Lide (Taylor and Francis, Boca Raton, 2009).
56. B. Weidenfeller, M. Höfer, and F. R. Schilling, Composites, Part A **35**, 423 (2004).
57. J. Wilson, Thermal Diffusivity. https://www.electronics-cooling.com/2007/08/thermal-diffusivity/. Cited 2019.
58. J. Blumm and A. Lindemann, High Temp.- High Pressures **35**, 6 (2003).
59. J. Blumm, A. Lindemann, M. Meyer, and C. Strasser, Int. J. Thermophys. **31**, 1919 (2010).